

## Supplementary Information

Tetraphenylethylene-based acylhydrazone gel for selective luminescent sensing

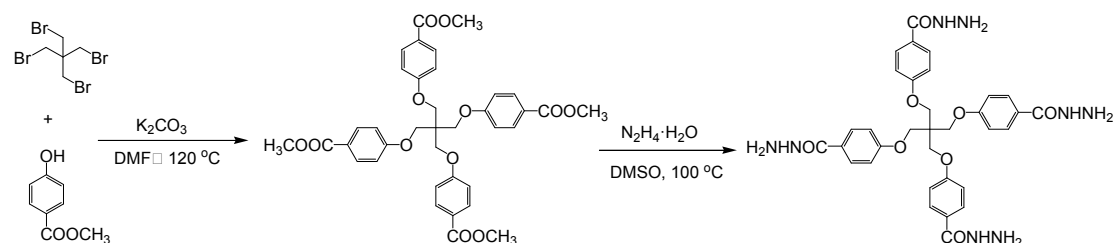
Haobin Fang, Guangmei Cai, Ya Hu and Jianyong Zhang\*

*Sun Yat-Sen University, MOE Laboratory of Polymeric Composite and Functional Materials, MOE Laboratory of Bioinorganic and Synthetic Chemistry, School of Materials Science and Engineering, Guangzhou 510275, China. Email: zhjyong@mail.sysu.edu.cn*

## Experimental

Chemicals and solvents were obtained from commercial sources and used as received without further purification unless otherwise stated. 1,1,2,2-tetrakis(4-formyl-(1,1'-biphenyl))ethene (TFBE)<sup>1</sup> was synthesized as reported previously. Adsorption measurements were performed using a Quantachrome Autosorb-iQ2 analyzer. Prior to analysis, the aerogel sample was degassed at 100 °C for 16 h to remove solvated molecules. NMR spectra were recorded on a Bruker Avance III 400 MHz spectrometer. <sup>13</sup>C Solid-state NMR spectrum was recorded on a Bruker AVANCE 400 Superconducting Fourier Transform Nuclear Magnetic Resonance Spectroscopy instrument. Scanning electron microscopy (SEM) and energy dispersive X-ray spectroscopy (EDX) were taken using a Quanta 400F scanning electron microscope with an Inca energy dispersive X-ray spectrometer or an Ultra-high Resolution FE-SEM SU8010 scanning electron microscope. Before measurement, the sample was dispersed in ethanol with the aid of sonication, put on aluminum foil, and sputter coated with gold. Transmission electron microscopy (TEM) investigations were carried out on a FEI Tecnai G2 Spirit 120 kV transmission electron microscope. The sample was dispersed in ethanol with the aid of sonication and mounted on a carbon coated copper grid. Powder X-ray diffraction data were collected on a Bruker Smartlab diffractometer. Thermo analyses were performed under N<sub>2</sub> atmosphere at a heating rate of 10 K min<sup>-1</sup> with a NETZSCH TG STA 449 F3 Jupiter system. Rheological measurements were carried out on a HAAKE MARS(III) rheometer at 298 K. The diameter of upper plate is 20 mm, and the distance between the lower and upper is 2.6-2.8 mm for tests. Infrared spectra were recorded on a Nicolet/Nexus 670 FT-IR spectrometer with KBr pellets in the range 4000 - 400 cm<sup>-1</sup>. The photoluminescence spectra were measured on Edinburgh FLS980 fluorescence spectrometer by a cuvette.

## Synthesis of acylhydrazide-terminated pentaerythritol (PAT)



PAT was synthesized from pentaerythritol tetra-p-methyl benzoate according to the published procedure.<sup>2</sup> Pentaerythritol tetra-p-methyl benzoate was synthesized from pentaerythritol tetrabromide and methyl 4-hydroxybenzoate.<sup>3</sup>

## Preparation of PAT-TFBE gel

PAT (0.135 g, 0.02 mmol) was dissolved in DMSO (0.5 mL) and TFBE (0.0149 g, 0.02 mmol) was in DMSO (0.5 mL) at 80 °C. The solutions were mixed at 80 °C and one drop of acetic acid (3 mol L<sup>-1</sup> in DMSO) was added. The reaction mixture was heated at 80 °C for 1 d to obtain a greenish yellow opaque gel. The resulting gel was further aged for 24 h. The gel was subsequently washed with DMSO at RT. DMSO was replaced every day by fresh solvent and solvent exchange was finished after three days. Then the gel was washed with EtOH for three days in similar way. The solvent in the exchanged gel was next extracted with subcritical CO<sub>2</sub>(l) (270 g) for 20 h in a 0.75 L high pressure stainless-steel Soxhlet extractor and the extraction temperature was kept at 35 °C (pressure 5.8 MPa). After the stainless-steel autoclave was depressurized slowly at RT for about 2-3 h to get the aerogel as yellow crushed solid (0.0225 g, 83%). Solid-state <sup>13</sup>C CP/MAS NMR (400 MHz):  $\delta$  162.9, 143.3, 133.1, 127.9, 116.0, 68.6, 47.7.

1 W. Luo, Y. Zhu, J. Zhang, J. He, Z. Chi, P. W. Miller, L. Chen and C. Y. Su, *Chem. Commun.*, 2014, **50**, 11942–11945.

2 Y.-Q. Lan, S.-L. Li, H.-L. Jiang and Q. Xu, *Chem. Eur. J.*, 2012, **18**, 8076-8083.

3 D. E Apostolides, C. S. Patrickios, E. Leontidis, M. Kushnirb and C. Wesdemiotis, *Polym. Int.*, 2014, **63**, 1558–1565.

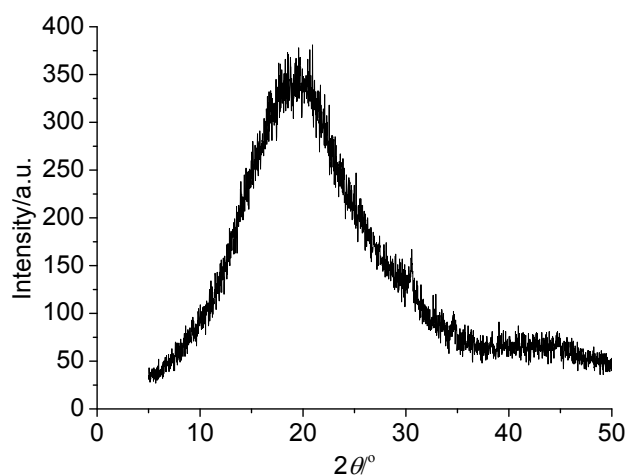


**Fig. S1** Powder X-ray diffraction patterns of PAT-TFBE aerogel.

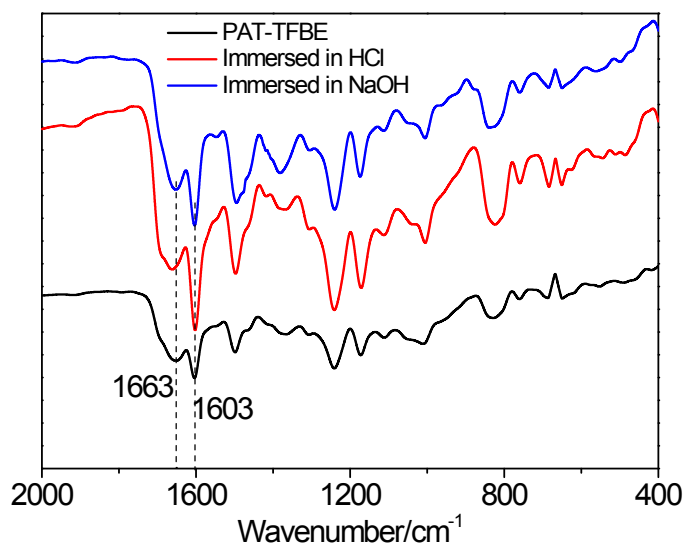


**Fig. S2** FT-IR spectra of PAT-TFBE wet gel, the gel immersed in HCl or NaOH aqueous solutions ( $3 \text{ mol L}^{-1}$ ).

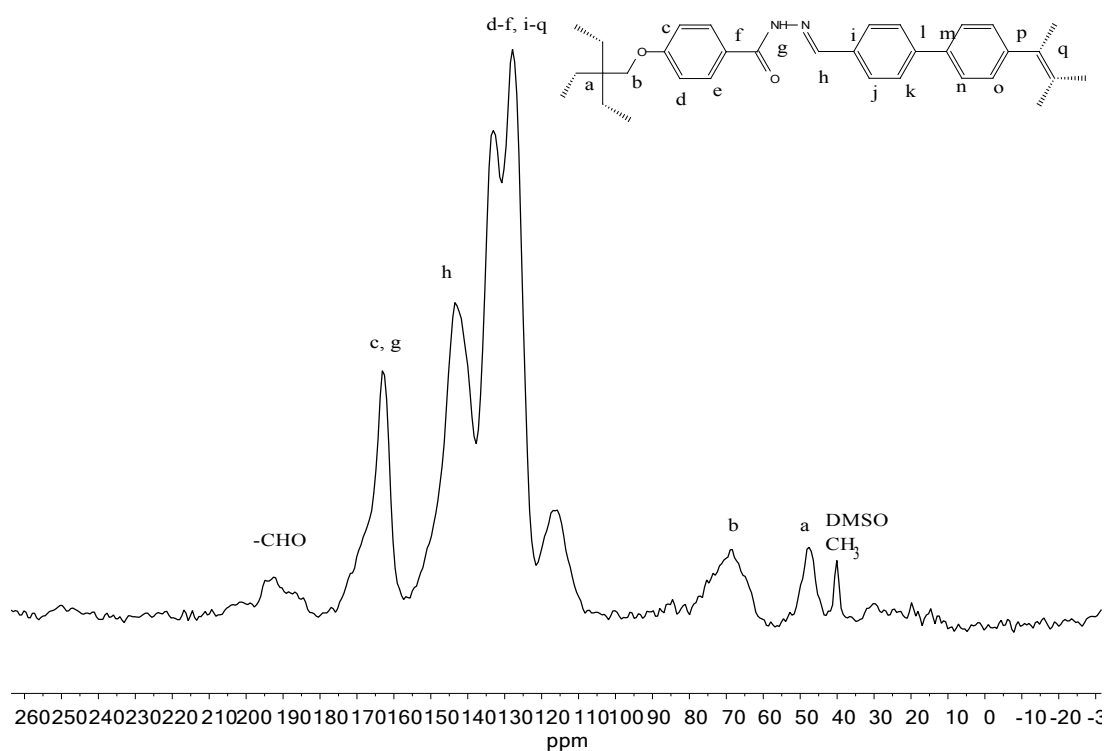


**Fig. S3** Solid-state  $^{13}\text{C}$  CP/MAS NMR spectrum of PAT-TFBE aerogel (400 MHz).

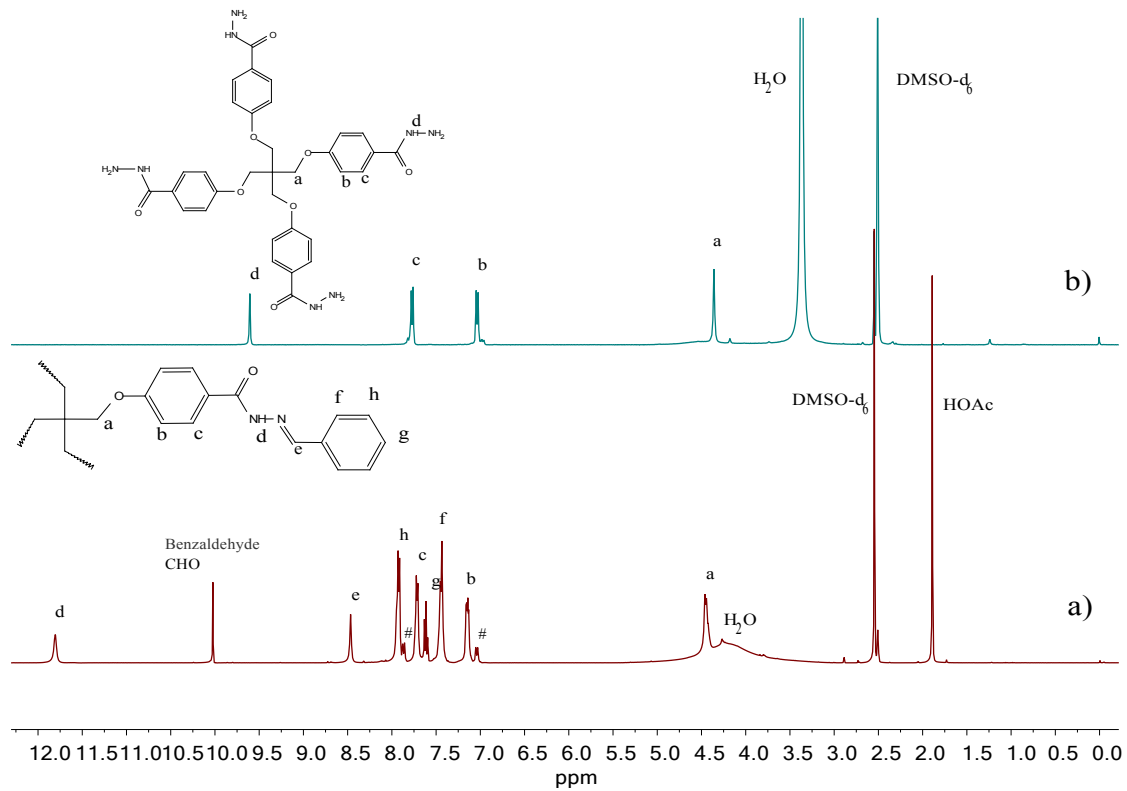


**Fig. S4** <sup>1</sup>H NMR spectra (400 MHz, 298 K) of a) reaction mixture of PAT and benzaldehyde in DMSO-d<sub>6</sub> (1:4,  $c_{PAT} = 1 \text{ mol L}^{-1}$ ) after reacting at 80 °C for 1 d, and b) PAT in DMSO-d<sub>6</sub>.

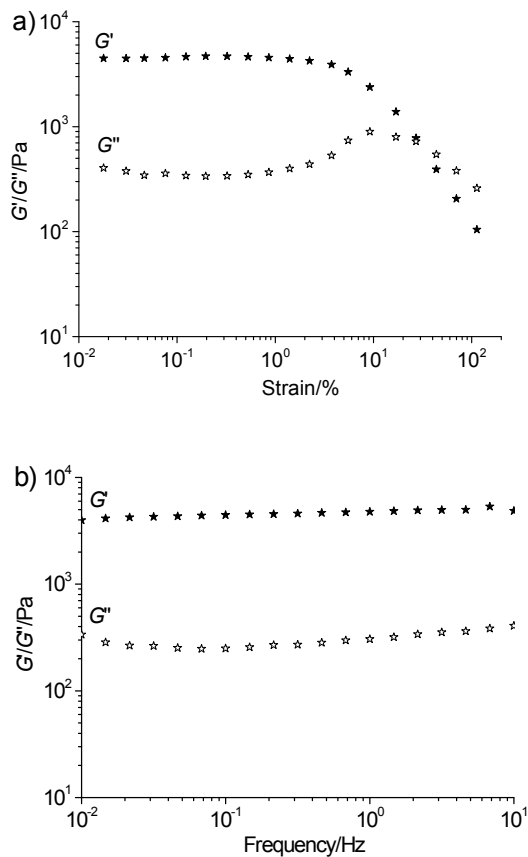


**Fig. S5** Rheological tests of PAT-TFBE gel, a) strain sweep at constant frequency of 1 Hz and b) frequency sweep at constant strain of 1%.

The gel was monitored as functions of shear strain and dynamic frequency at room temperature to determine the linear viscoelastic regime. For strain sweep test, the frequency is 1 Hz and the range of strain is from 0.01% to 100%. For frequency sweep, the strain of the gel is 1% and the range of frequency is from 0.01 Hz to 10 Hz. For strain sweep test, below the strain of 2% as the upper limit of the linear viscoelastic regime, the modulus kept constant approximately. The average storage modulus ( $G'$ ) was higher than the loss modulus ( $G''$ ), indicating dominant elastic characters of the gels. With the strain increases gradually,  $G'$  fell sharply, whereas the  $G''$  firstly increased and then fell, indicating that the gels began to breakup partially. Above the critical value of strain approximately 30%, the  $G''$  became greater than the  $G'$ , which indicate that the network of the gels was completely destroyed.

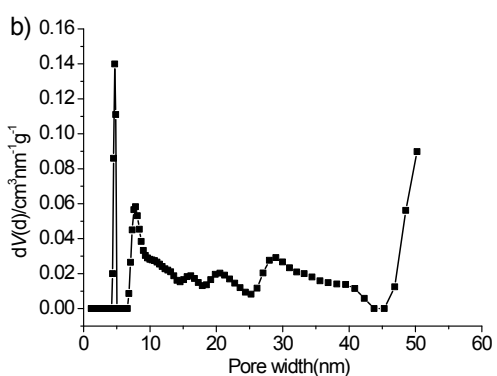
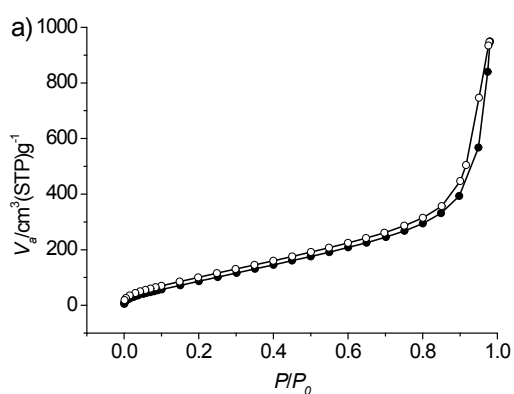


**Fig. S6** a)  $N_2$  adsorption (closed symbols) /desorption (open symbols) isotherms for PAT-TFBE aerogel at 77 K, b) pore size distribution estimated by using quenched solid density functional theory (QSDFT) (Model:  $N_2$  at 77 K on carbon (cylindr./sphere pores, QSDFT adsorption branch).

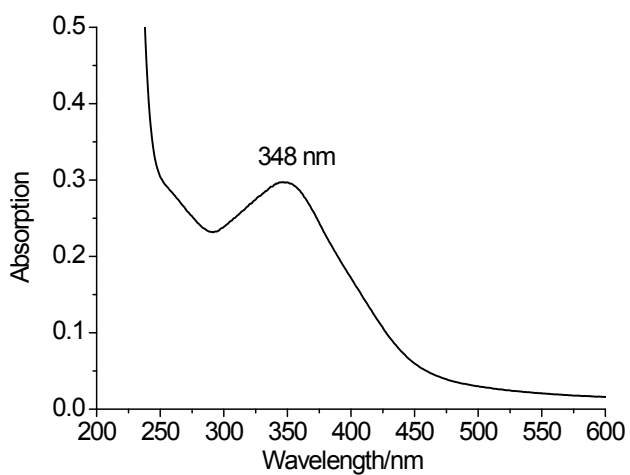


**Fig. S7** UV-vis absorption spectrum of PAT-TFBE gel dispersion in water ( $1 \times 10^{-5}$  mol  $L^{-1}$  based on PAT or TFBE).

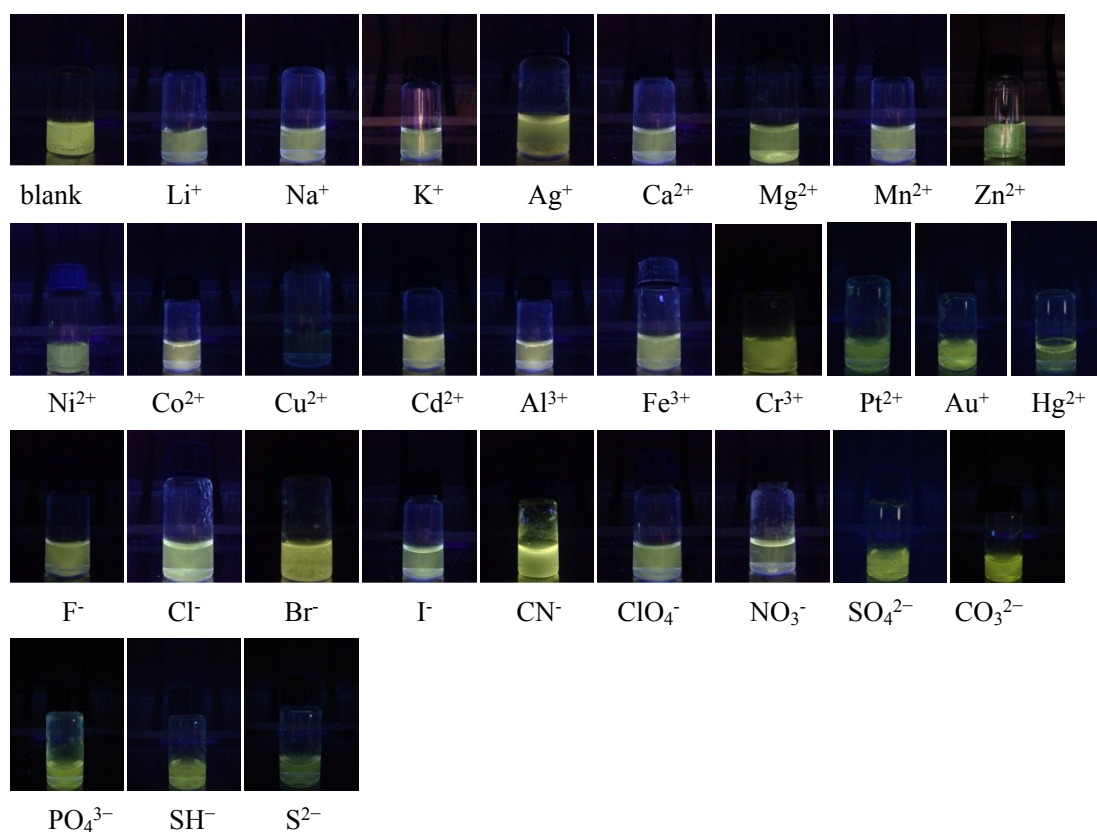


**Fig. S8** Photographic images of the response of the PAT-TFBE gel dispersed in water (3 mL,  $1 \times 10^{-5}$  mol L<sup>-1</sup> based on PAT or TFBE) to various cation aqueous solutions (0.3 mL,  $4 \times 10^{-4}$  mol L<sup>-1</sup>, nitrate salt except Au<sup>+</sup> in AuCl) and anion aqueous solutions (0.3 mL,  $4 \times 10^{-4}$  mol L<sup>-1</sup>, F<sup>-</sup>, Cl<sup>-</sup>, Br<sup>-</sup>, I<sup>-</sup>, CN<sup>-</sup>, ClO<sub>4</sub><sup>-</sup> and NO<sub>3</sub><sup>-</sup> tetrabutylammonium salt and SO<sub>4</sub><sup>2-</sup>, CO<sub>3</sub><sup>2-</sup>, PO<sub>4</sub><sup>3-</sup>, SH<sup>-</sup> and S<sup>2-</sup>, sodium salt) under 365 nm UV illumination.

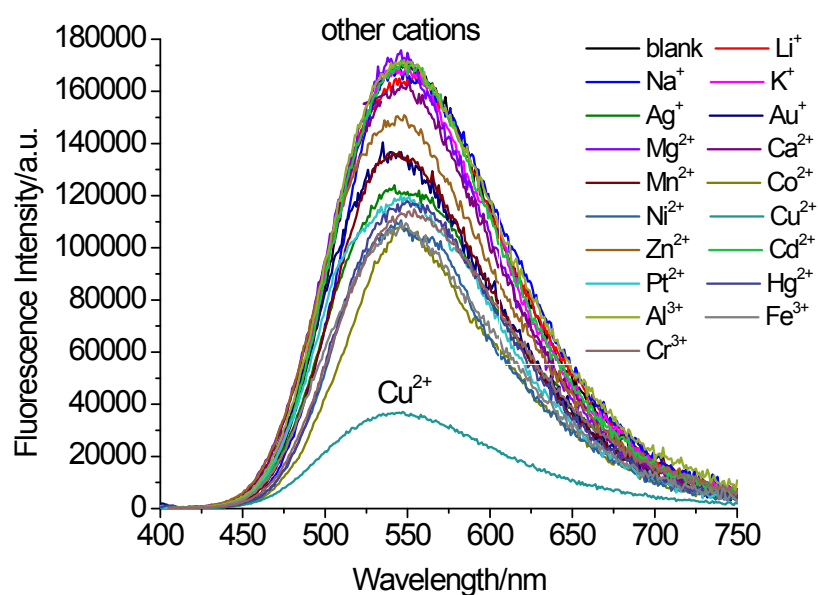


**Fig. S9** Changes in fluorescence spectra ( $\lambda_{\text{ex}} = 350$  nm) of PAT-TFBE dispersed in water (3 mL,  $1.0 \times 10^{-5}$  mol L<sup>-1</sup> based on PAT or TFBE) to a specific cation aqueous solution (0.03 mL,  $4 \times 10^{-3}$  mol L<sup>-1</sup>, nitrate salt except Au<sup>+</sup> in AuCl).

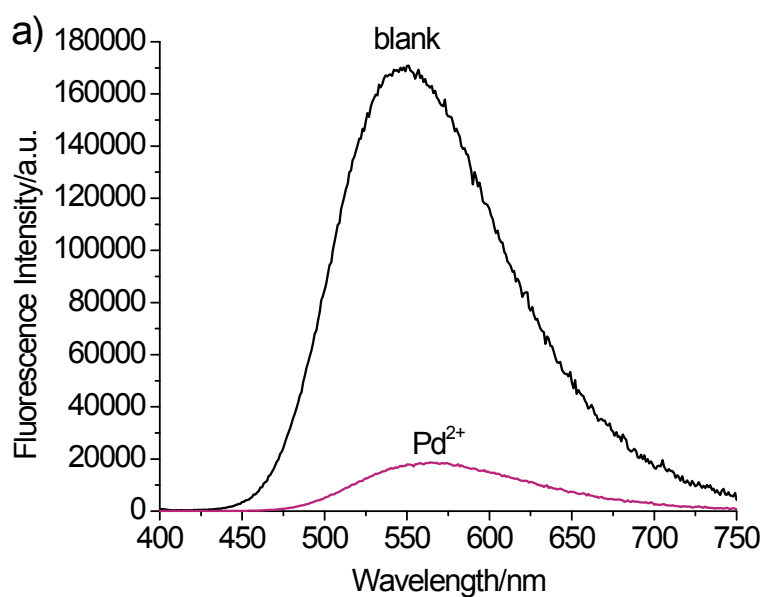


**Fig. S10** a) Changes in fluorescence spectra ( $\lambda_{\text{ex}} = 350 \text{ nm}$ ) of PAT-TFBE dispersed in water (3 mL,  $1.0 \times 10^{-5} \text{ mol L}^{-1}$  based on PAT or TFBE) to Pd<sup>2+</sup> aqueous solution (0.06 mL,  $4 \times 10^{-3} \text{ mol L}^{-1}$ , nitrate salt), photographic images of b) the PAT-TFBE gel dispersed in water and e) PAT-TFBE gel dispersion (3 mL,  $1.0 \times 10^{-5} \text{ mol L}^{-1}$ ) in the presence of Pd(NO<sub>3</sub>)<sub>2</sub> aqueous solutions (0.06 mL,  $4 \times 10^{-3} \text{ mol L}^{-1}$ ) in daylight, and d) under 365 nm UV illumination.

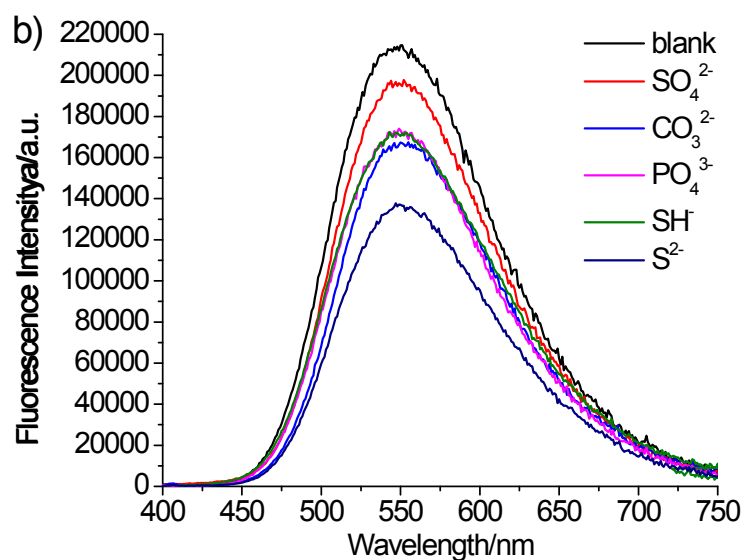
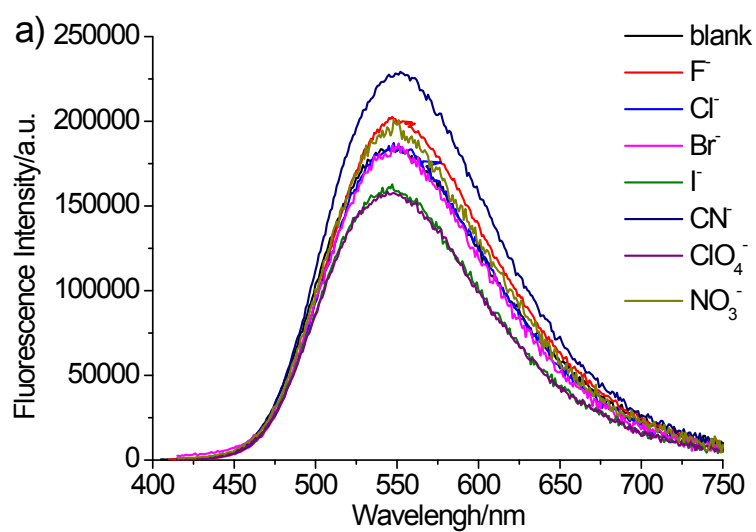


**Fig. S11** Changes in fluorescence spectra ( $\lambda_{\text{ex}} = 350 \text{ nm}$ ) of PAT-TFBE dispersed in water (3 mL,  $1.0 \times 10^{-5} \text{ mol L}^{-1}$  based on PAT or TFBE) to a specific anion aqueous solution (0.03 mL,  $4 \times 10^{-3} \text{ mol L}^{-1}$ ), a) F<sup>-</sup>, Cl<sup>-</sup>, Br<sup>-</sup>, I<sup>-</sup>, CN<sup>-</sup>, ClO<sub>4</sub><sup>-</sup> and NO<sub>3</sub><sup>-</sup>, tetrabutylammonium salt, b) SO<sub>4</sub><sup>2-</sup>, CO<sub>3</sub><sup>2-</sup>, PO<sub>4</sub><sup>3-</sup>, SH<sup>-</sup> and S<sup>2-</sup>, sodium salt.

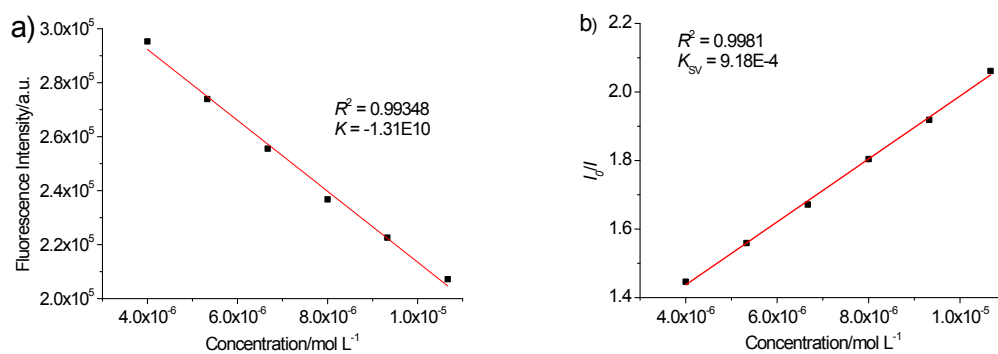


**Fig. S12** a) Curve fitting of the fluorescence intensity of PAT-TFBE gel dispersion in water vs.  $\text{Cu}^{2+}$  concentration, and b) Stern-Volmer plot of the relative fluorescence intensity of PAT-TFBE gel dispersion in water vs.  $\text{Cu}^{2+}$  concentration.

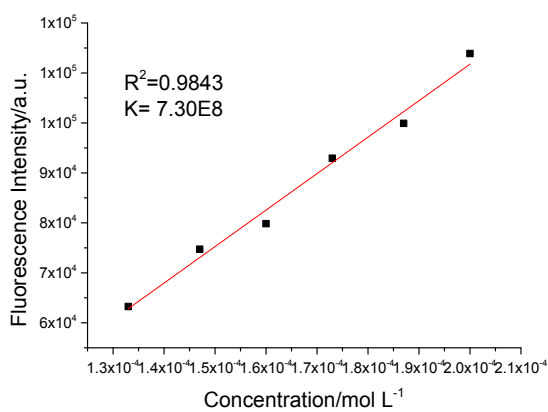


**Fig. S13** Curve fitting of the fluorescence intensity of PAT-TFBE-Cu vs.  $\text{CN}^-$  concentration in aqueous solution.

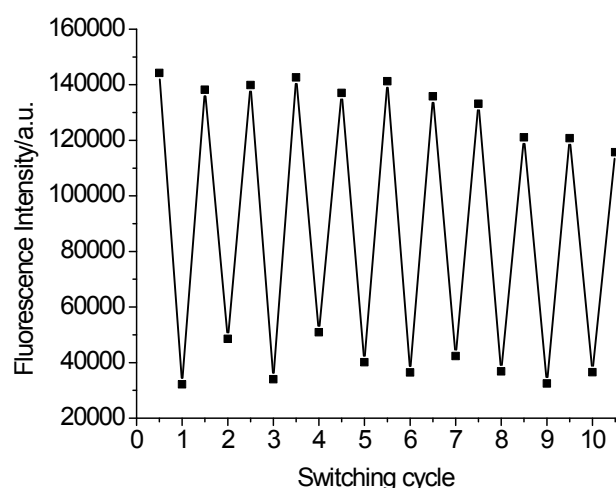


**Fig. S14** Fluorescence switching of the PAT-TFBE gel aqueous dispersion (3.0 mL,  $1.0 \times 10^{-5}$  mol L $^{-1}$  based on PAT) by alternating addition of Cu $^{2+}$  aqueous solution (0.01 mL,  $1.2 \times 10^{-2}$  mol L $^{-1}$ , nitrate salt) to the gel aqueous dispersion and CN $^{-}$  (0.01 mL,  $6.0 \times 10^{-2}$  mol L $^{-1}$ , tetrabutylammonium salt) aqueous solution successively ( $\lambda_{\text{ex}} = 350$  nm, the maximum fluorescent intensities at 550 nm are recorded and plotted).

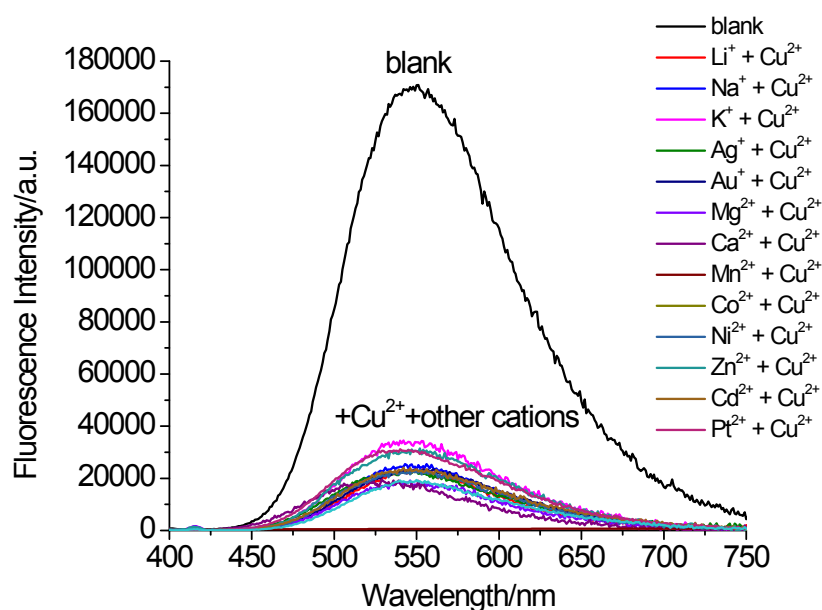


**Fig. S15** Fluorescence competition experiments of PAT-TFBE to metal ions ( $\lambda_{\text{ex}} = 350$  nm). Cu $^{2+}$  aqueous solution (0.06 mL,  $4.0 \times 10^{-3}$  mol L $^{-1}$ ) was added to PAT-TFBE gel dispersion in water (3 mL,  $1.0 \times 10^{-5}$  mol L $^{-1}$  based on PAT or TFBE) in the presence of miscellaneous cation (0.06 mL,  $4.0 \times 10^{-3}$  mol L $^{-1}$ , nitrate salt except Au $^{+}$  in AuCl).

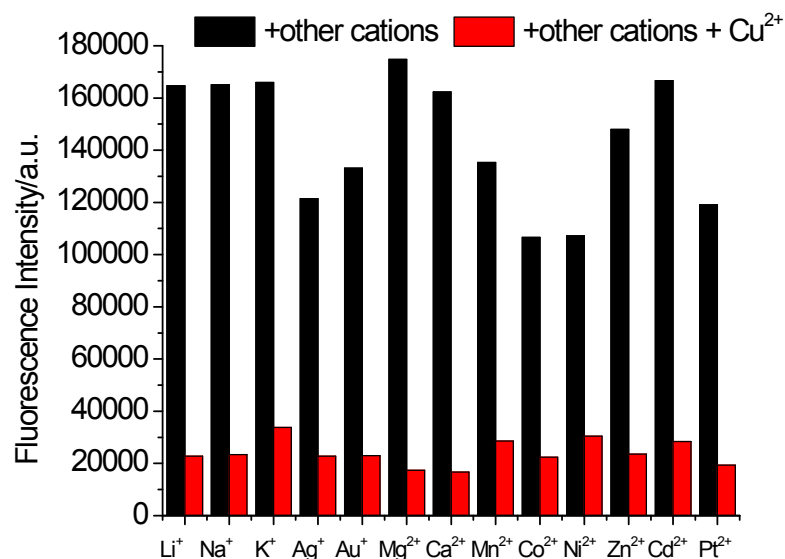


**Fig. S16** Fluorescence competition experiments of PAT-TFBE gel dispersion in water (3 mL,  $1.0 \times 10^{-5}$  mol L<sup>-1</sup> based on PAT or TFBE) to various metal ions with 350 nm excitation. The black bars represent the fluorescence of PAT-TFBE in the presence of miscellaneous cations (0.06 mL,  $4.0 \times 10^{-3}$  mol L<sup>-1</sup>), and the red bars represent the fluorescence of the above mixture upon subsequent addition of Cu<sup>2+</sup> (0.06 mL,  $4.0 \times 10^{-3}$  mol L<sup>-1</sup>).

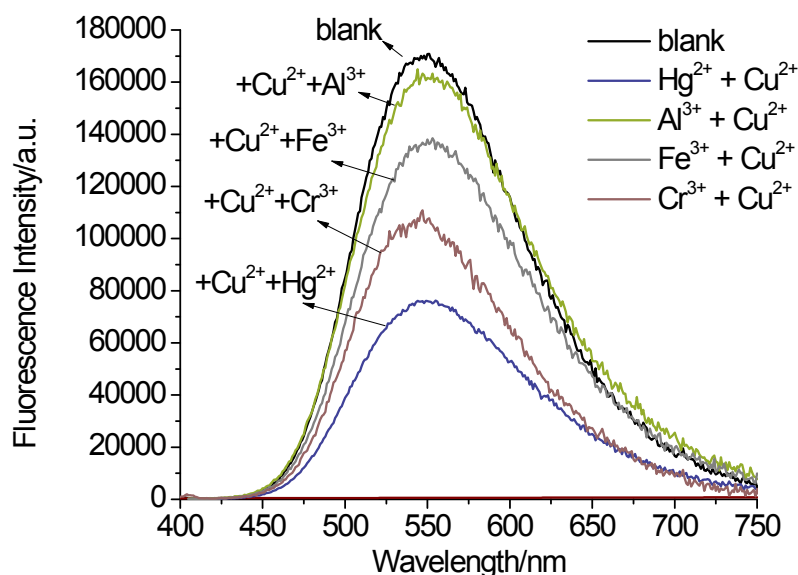


**Fig. S17** Fluorescence competition experiments of PAT-TFBE to metal ions ( $\lambda_{\text{ex}} = 350$  nm). Cu<sup>2+</sup> aqueous solution (0.06 mL,  $4.0 \times 10^{-3}$  mol L<sup>-1</sup>, nitrate salt) was added to PAT-TFBE gel dispersion in water (3 mL,  $1.0 \times 10^{-5}$  mol L<sup>-1</sup> based on PAT or TFBE) in the presence of Hg<sup>2+</sup>, Al<sup>3+</sup>, Fe<sup>3+</sup> or Cr<sup>3+</sup> (0.06 mL,  $4.0 \times 10^{-3}$  mol L<sup>-1</sup>, nitrate salt).

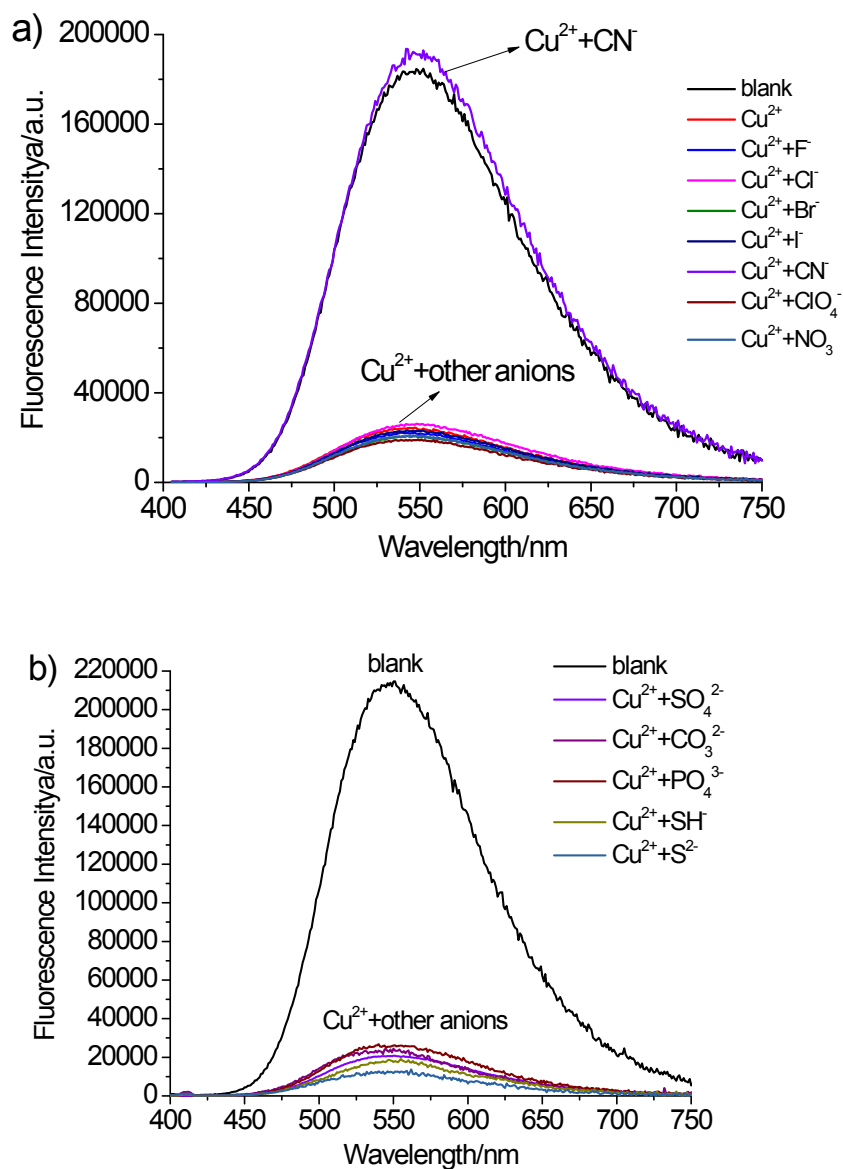


**Fig. S18** Changes in fluorescence spectra of PAT-TFBE gel dispersed in water (3 mL,  $1.0 \times 10^{-5}$  mol L<sup>-1</sup> based on PAT or TFBE) in present of Cu<sup>2+</sup> aqueous solution (0.06 mL,  $4.0 \times 10^{-3}$  mol L<sup>-1</sup>) (PAT-TFBE-Cu) to a subsequently added specific anion aqueous solution (0.3 mL,  $4.0 \times 10^{-3}$  mol L<sup>-1</sup>) with 350 nm excitation, a) F<sup>-</sup>, Cl<sup>-</sup>, Br<sup>-</sup>, I<sup>-</sup>, CN<sup>-</sup>, ClO<sub>4</sub><sup>-</sup> and NO<sub>3</sub><sup>-</sup>, tetrabutylammonium salt, b) SO<sub>4</sub><sup>2-</sup>, CO<sub>3</sub><sup>2-</sup>, PO<sub>4</sub><sup>3-</sup>, SH<sup>-</sup> and S<sup>2-</sup>, sodium salt.

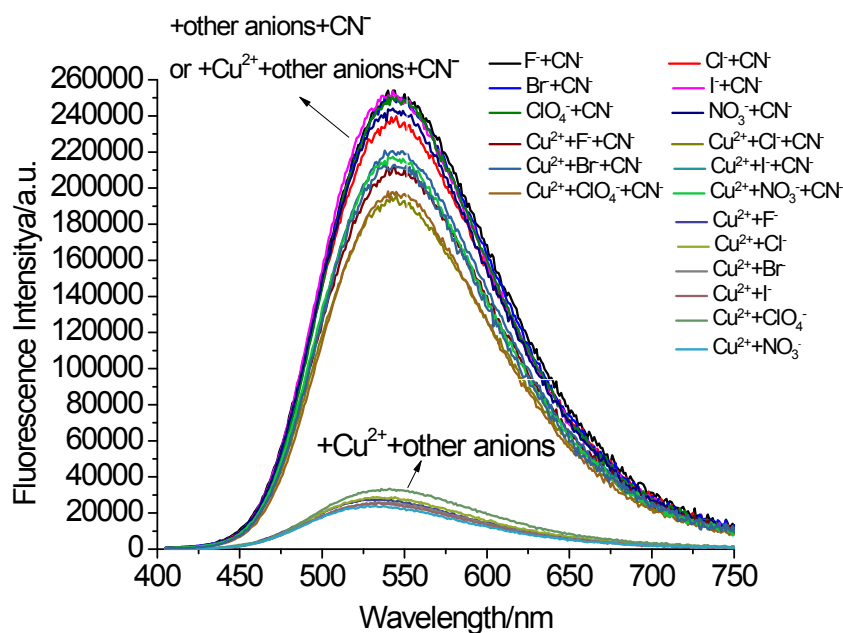


**Fig. S19** Fluorescence competition experiments of PAT-TFBE-Cu (0.06 mL,  $4 \times 10^{-3}$  mol L<sup>-1</sup> based on Cu<sup>2+</sup>) in the presence of various anions ( $\lambda_{\text{ex}} = 350$  nm). CN<sup>-</sup> aqueous solution (0.3 mL,  $4.0 \times 10^{-3}$  mol L<sup>-1</sup>) was subsequently added to PAT-TFBE or PAT-TFBE-Cu in the presence of miscellaneous anion aqueous solution (0.3 mL,  $4.0 \times 10^{-3}$  mol L<sup>-1</sup>, F<sup>-</sup>, Cl<sup>-</sup>, Br<sup>-</sup>, I<sup>-</sup>, ClO<sub>4</sub><sup>-</sup> or NO<sub>3</sub><sup>-</sup>, tetrabutylammonium salt).

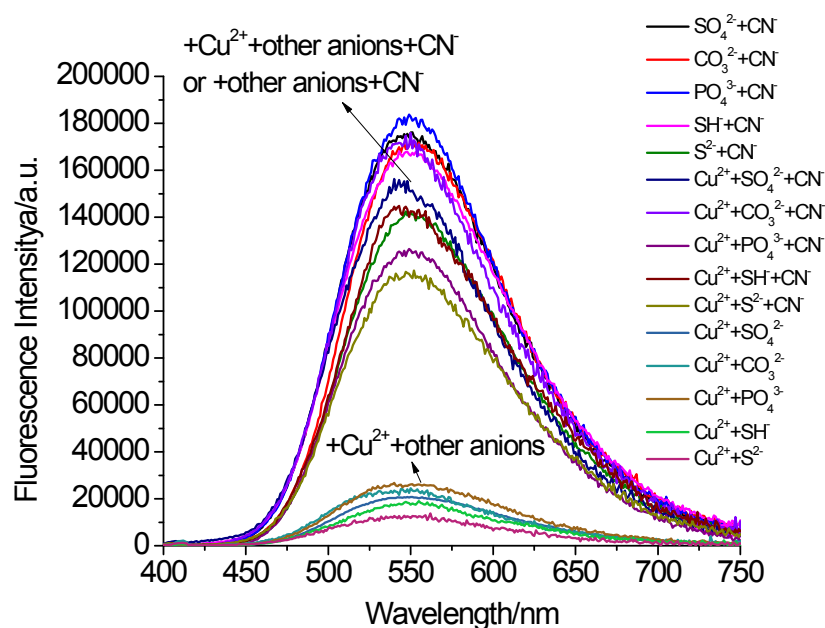


**Fig. 20** Fluorescence competition experiments of PAT-TFBE-Cu (0.06 mL,  $4 \times 10^{-3}$  mol L<sup>-1</sup> based on Cu<sup>2+</sup>) in the presence of various anions ( $\lambda_{\text{ex}} = 350$  nm). CN<sup>-</sup> aqueous solution (0.3 mL,  $4.0 \times 10^{-3}$  mol L<sup>-1</sup>, tetrabutylammonium salt) was subsequently added to PAT-TFBE or PAT-TFBE-Cu in the presence of miscellaneous anion aqueous solution (0.3 mL,  $4.0 \times 10^{-3}$  mol L<sup>-1</sup>, SO<sub>4</sub><sup>2-</sup>, CO<sub>3</sub><sup>2-</sup>, PO<sub>4</sub><sup>3-</sup>, SH<sup>-</sup> or S<sup>2-</sup>, sodium salt).

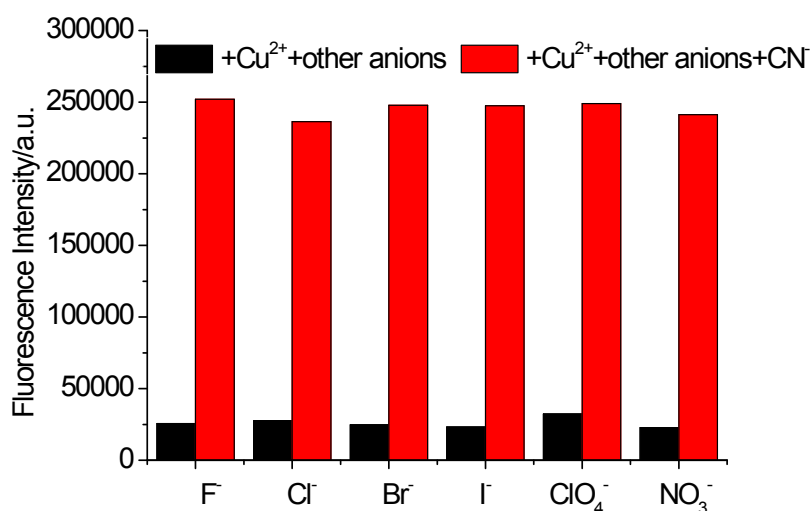


**Fig. S21** Fluorescence competition experiments of PAT-TFBE-Cu to various anions with 350 nm excitation. The black bars represent the fluorescence of PAT-TFBE-Cu in the presence of F<sup>-</sup>, Cl<sup>-</sup>, Br<sup>-</sup>, I<sup>-</sup>, ClO<sub>4</sub><sup>-</sup> or NO<sub>3</sub><sup>-</sup> anions aqueous solution (0.3 mL, 4.0×10<sup>-3</sup> mol L<sup>-1</sup>, tetrabutylammonium salt), the red bars represent the fluorescence of the above mixture upon sub-sequent addition of CN<sup>-</sup> (0.3 mL, 4.0×10<sup>-3</sup> mol L<sup>-1</sup>).

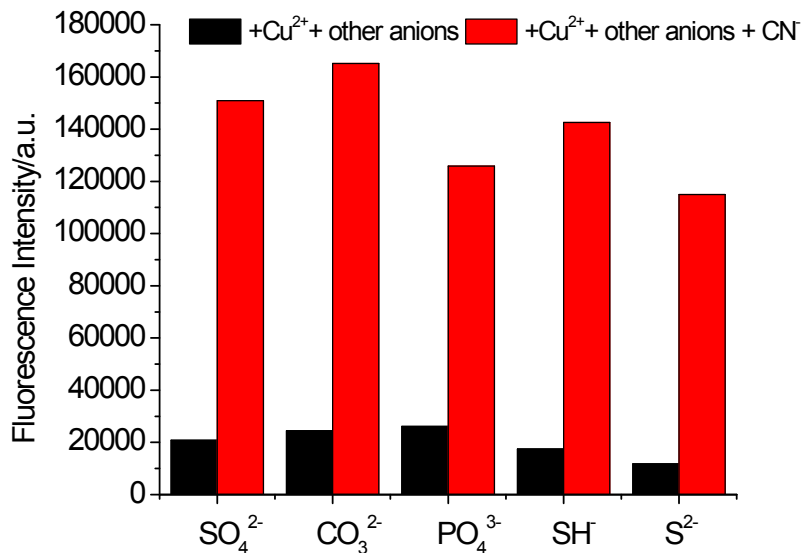


**Fig. S22** Fluorescence competition experiments of PAT-TFBE-Cu to various anions with 350 nm excitation. The black bars represent the fluorescence of PAT-TFBE-Cu in the presence of SO<sub>4</sub><sup>2-</sup>, CO<sub>3</sub><sup>2-</sup>, PO<sub>4</sub><sup>3-</sup>, SH<sup>-</sup> or S<sup>2-</sup> aqueous solutions (0.3 mL, 4×10<sup>-3</sup> mol L<sup>-1</sup>, sodium salt), the red bars represent the fluorescence of the above mixture upon subsequent addition of CN<sup>-</sup> (0.3 mL, 4.0×10<sup>-3</sup> mol L<sup>-1</sup>).

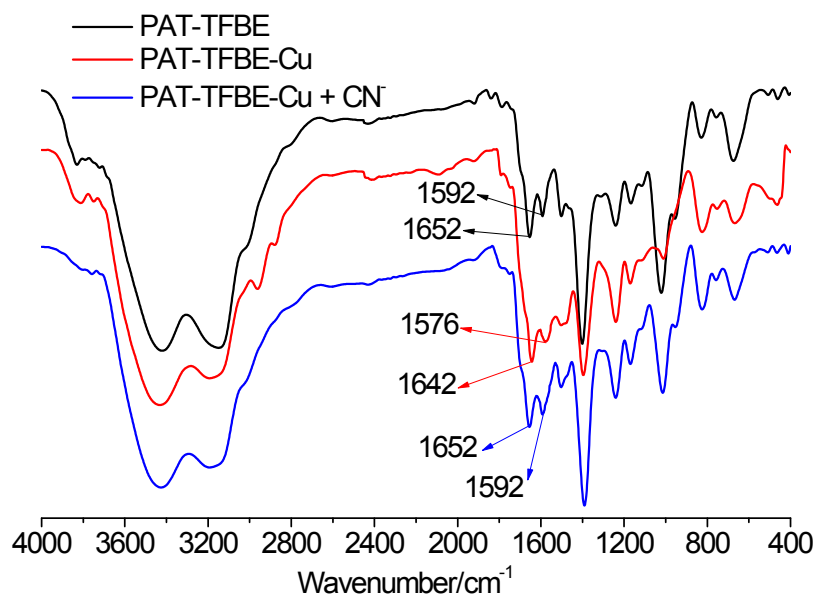


**Fig. S23** FT-IR spectra of PAT-TFBE wet gel, the gel immersed by  $\text{Cu}^{2+}$  aqueous solution ( $0.3 \text{ mL}$ ,  $4.0 \times 10^{-3} \text{ mol L}^{-1}$ ) for 1 d, then the above gel immersed by  $\text{CN}^-$  aqueous solution ( $0.6 \text{ mL}$ ,  $4.0 \times 10^{-3} \text{ mol L}^{-1}$ ) for 1 d.

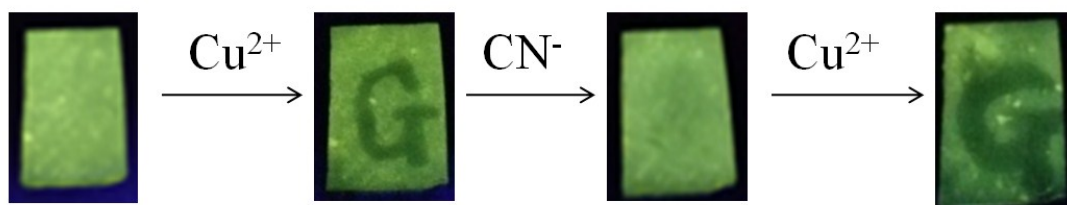


**Fig. S24** Photographs of fluorescent test of PAT-TFBE gel aqueous dispersion ( $1.0 \times 10^{-4} \text{ mol L}^{-1}$  based on PAT or TFBE) coated on silica gel G thin-layer plate for  $\text{Cu}^{2+}$  and  $\text{CN}^-$  ( $4 \times 10^{-3} \text{ mol L}^{-1}$ ) detection under 365 nm UV radiation.